DOI: https://doi.org/10.3986/ac.v54i1.14017

MODELLING FLOW AND TRANSPORT TO ASSESS THE INFLUENCE OF SUBSURFACE GEOMETRY ON ALPINE KARST AQUIFER VULNERABILITY

MODELIRANJE PRETOKA VODE IN PRENOSA ZA PRESOJO VPLIVA GEOMETRIJE PODPOVRŠINSKIH PLASTI NA RANLJIVOST ALPSKOKRAŠKEGA VODONOSNIKA

Barbara FLECK[1*], Lukas PLAN[2], Bernhard GRASEMANN[1] & Cyril MAYAUD[3,4]

Abstract UDC 556.1:556.33:551.44

Barbara Fleck, Lukas Plan, Bernhard Grasemann & Cyril Mayaud: Modelling flow and transport to assess the influence of subsurface geometry on Alpine karst aquifer vulnerability

Karst areas are highly susceptible to contamination due to rapid recharge and throughflow caused by their heterogeneous structure with unknown networks of conduits embedded in a matrix of low conductivity. Vulnerability methods have been used to ensure adequate protection of drinking water resources. However, most of the studies assessing the vulnerability of karst aquifers consider it as a constant value in time and, therefore, under special hydrological conditions in space, which is an oversimplification of reality. In this work, the behaviour of an Alpine karst system characterised by rapid flow and transfer through vertical shafts has been studied by discrete numerical modelling using MODFLOW 6. Six numerical models have been designed with the aim of representing simple common geometrical configurations found in Alpine karst systems. These models simulate how the flow and transport response at the system outlet is influenced by the aquifer geometry and recharge conditions. The results confirm that the arrival of the tracer at the spring strongly depends on the conduit geometry and the recharge conditions. This demonstrates that karst aquifer vulnerability cannot be defined as a constant value but should be specifically assessed depending on the spatio-temporal conditions.

Keywords: Alpine karst system, numerical flow and transport modelling, vulnerability, overflow, MODFLOW 6.

Izvleček UDK 556.1:556.33:551.44

Barbara Fleck, Lukas Plan, Bernhard Grasemann & Cyril Mayaud: Modeliranje pretoka vode in prenosa za presojo vpliva geometrije podpovršinskih plasti na ranljivost alpskokraškega vodonosnika

Kraška območja so zelo dovzetna za onesnaženje zaradi hitrega napajanja in pretoka, kar omogoča njihova heterogena struktura z neznanimi omrežji kanalov, ki so del matrike z nizko prevodnostjo. Za zagotavljanje ustreznega varstva virov pitne vode so bile uporabljene metode proučevanja ranljivosti. Vendar večina študij, ki proučuje ranljivost kraških vodonosnikov, to obravnava kot časovno konstantno vrednost in kot prostor v posebnih hidroloških razmerah, kar je prevelika poenostavitev realnega stanja. V tem članku so bile z diskretnim numeričnim modeliranjem s programom MODFLOW 6 proučene lastnosti alpskokraškega sistema, za katerega je značilen hiter pretok vode po navpičnih jaških. Oblikovanih je bilo šest numeričnih modelov, katerih cilj je predstaviti preproste običajne geometrijske konfiguracije, ki jih najdemo v sistemih alpskega krasa. Ti modeli simulirajo, kako geometrija vodonosnika in značilnosti napajanja vplivajo na pretok in prenos na iztoku. Rezultati potrjujejo, da je prihod sledila v izvir močno odvisen od geometrije kanalov in značilnosti napajanja. To dokazuje, da ranljivosti kraških vodonosnikov ni mogoče opredeliti kot konstantno vrednost, temveč jo je treba proučevati specifično glede na prostorsko-časovne razmere.

Ključne besede: sistem alpskega krasa, numerično modeliranje pretoka in prenosa, ranljivost, preplavljanje, MODFLOW 6.

[1] University of Vienna, Department of Geology, Josef Holaubek-Platz 2, 1090 Vienna, Austria
[2] Karst- and Cave Group, Natural History Museum Vienna, Burgring 7, 1010 Vienna, Austria
[3] ZRC SAZU, Karst Research Institute, Titov trg 2, 6230 Postojna, Slovenia
[4] UNESCO Chair on Karst Education, University of Nova Gorica, Glavni trg 8, 5271 Vipava, Slovenia

Received/Prejeto: 2. 12. 2025

1. INTRODUCTION

Karst areas cover approximately 12-15% of the Earth's ice-free surface and provide drinking water to 20-25% of the world population (Ford & Williams, 2007; Chen et al., 2017). In Austria their contribution is even higher and reaches 50% of the total drinking water supply (Kralik, 2001). A good example is the capital Vienna (1.9 million inhabitants), which receives 95% of its water from large karst springs located at the foot of the Hochschwab, Schneealpe, Rax, and Schneeberg Mountains (Plan et al., 2010). The recharge areas of these springs are characterised by a vadose zone up to 1.5 km thick where flow through vertical shafts prevails until reaching the phreatic zone. Such configuration is common in Alpine karst systems, and is also observed in Croatia (Stroj & Paar, 2019), France (Blavoux et al., 1992), Germany (Lauber & Goldscheider, 2014), Italy (Sauro et al., 2013), Slovenia (Gabrovšek et al., 2023), Spain (Ballesteros et al., 2015) and Switzerland (Jeannin, 2016). Generally, the hydrogeological characterization of karst aquifers is considered as challenging (Bakalowicz, 2005). Indeed, the water velocity might be very fast and transmit the contaminants to the spring rapidly (Petrič et al., 2018) without benefiting from filtration processes commonly taking place in porous aquifers. In addition, long-term contamination is possible due to the retention capacity of the matrix system (Maloszewski et al., 2002), while the aquifer boundaries can be temporarily modified by large fluctuations of hydraulic head (Blatnik et al., 2019). Then, processes such as inter-catchment flow and overflow might occur (Wagner et al., 2013; Mayaud et al., 2014; Koit et al., 2017; Plan et al., 2023), connecting the aquifer to its neighbouring recharge areas, which might be under different contamination backgrounds (Ravbar et al., 2011). This adds a supplementary difficulty to ensure a proper characterization of the aquifer before planning an adequate protection of the available water resources (Ravbar et al., 2023).

For all these reasons, vulnerability mapping methods have been developed to protect the karst aquifers since the end of the 90's (e.g., Doerfliger et al., 1999; Goldscheider et al., 2000; Zwahlen, 2004; Ravbar & Goldscheider, 2009; Kavouri et al., 2011; Živanović et al., 2016). All these methods are based on GIS where the subsurface conduit geometry is not considered, while most of them also have a vulnerability constant in time. Under special hydrological conditions like floods the catchment areas can change and thus the vulnerability of these parts changes as well. This is an approximation of reality, as changing hydrogeological conditions and the geometry of the conduit system might influence the vulnerability. Thus, the use of a numerical groundwater flow and transport model would be necessary to assess how the vulnerability may change in karst aquifers.

The aim of this work is to investigate how the flow and transport signals registered at the spring might be influenced by the conduit geometry and recharge conditions inside an Alpine karst massif. To do so, distributed numerical modelling is employed using simple numerical settings containing typical geometrical features that might be encountered in deep Alpine caves. These features are tested to see their effect on the flow and transport response.

2. STATE OF THE ART AND METHOD

Conversely to other karst areas, distributed numerical modelling has been rarely employed to investigate the hydrology of Alpine karst systems (Kavousi et al., 2020). The main reasons are related to:

1. In many Alpine systems information on the geometrical structure of both the vadose and phreatic zones remains scarce. As the exploration of the caves located inside Alpine karst systems is challenging due to often more than 100 m shafts, many of them are not mapped nor fully explored. Therefore, their geometrical characterization relies solely on the extrapolation of the information available on the surface and at the system outlets. While lumped parameters models proved to be successful to simulate the hydrology at both, sections of vadose cave (Kaminsky et al., 2021) or the whole catchment scale (Fleury et al., 2007), they are unable to consider an accurate geometry of the conduit network, and are not appropriate for the purpose of this work.
2. An intricate difficulty of the distributed models to properly consider the physics governing flow and transport in Alpine karst systems. Indeed, the successions of cascading shafts with permanent and intermittent flow implies an almost sub-vertical hydraulic gradient, which is numerically very challenging to be computed. In addition, the transfer of water through the vadose zone is governed by unsaturated flow, while

the phreatic zone is under turbulent flow. Authors such as Kaufman (2003), Kordilla et al. (2012), or Dal Soglio et al. (2020) already considered unsaturated flow successfully at both local and catchment scales. In addition, studies of speleogenesis can also provide information on the underground structure of an aquifer (e.g. Perne et al., 2014) showed the evolution of a sub-vertical karst network using a speleogenesis model that simulates the transition from a pressurised flow to a free surface flow. But still its wider application remained not so much implemented, mostly due to numerical limitations and the risk of equifinality on the results. Therefore, the use of a more simplified modelling approach appears to be necessary.

3. The quasi-absence of reliable hydrogeological data from inside the karst massif, which prevents having any relevant information on the fluctuation of the water level upon time and its reaction to flood events. Indeed, monitoring the hydrology of both the phreatic and vadose zones has been rarely implemented (Stroj & Paar, 2019). There are some exceptions such as the Hölloch (Muotatal, Switzerland), a cave with mainly phreatic flow and conduit dominated structure in the lower section, could be simulated satisfactorily by Jeannin (2001), using turbulent flow. But often the lack of knowledge on the aquifer structure prevents comparing the model geometry with the real conduit geometry. Thus, distributed numerical models are only used in an interpretative way to understand the effect of a particular geometry on the modelled result.

Because of these limitations, the modelling approach selected for this work needs to stay very simple, focusing on simulating the sole effect of the conduit geometry on the spring response, rather than correctly reproducing the physics governing flow in Alpine karst systems.

To achieve this purpose, the open access software MODFLOW 6 (Langevin, 2017) was selected. The simulations use different hydraulic conductivities to represent matrix and conduits which is called equivalent porous media (EPM). The EPM can be used to simulate moderately to highly karstified systems with unknown geometry of the karst aquifer network (Teutsch & Sauter, 1998; De Waele & Gutiérrez, 2022).

With MODFLOW 6 only Darcian flow is implemented, which means that the flow in the model is only laminar.

Modflow 6 with EPM was used because it is suitable for: (1) simulation of processes in the vadose zone such as shown in the conceptual model used in this work (Figure 2); (2) modelling of unsaturated flow in vertical structures and (3) regional scale applications (Jourde et al., 2023).

Earlier versions of MODFLOW considering either turbulent flow such as CFP (Shoemaker al., 2008; Reimann et al., 2014), MODFLOW-USG (Panday et al., 2013; Duran & Gill, 2021) or non-linear flow such as NLFP (Mayaud et al., 2015) were not selected, as it was expected that they would fail to reach convergence and to our knowledge are not able to simulate transport. MODFLOW 6 is seen as a good option as the approach to construct the model remains rather simple. In addition, the MODFLOW programs are known for their compatibility with transport subroutines such as MT3DMS or the transport subroutine of MODFLOW 6 that are known to simulate transport processes very accurately (Panday, 2018). For this work, the Python package FloPy (Bakker et al., 2016) was used to build the models.

MODFLOW and Python are open-source products. MODFLOW 6 is the latest version of the program that has been developed since 1984 (Langevin et al., 2017). This version is realised in an object-oriented programming style that allows using a modular structure. The Ground Water Flow (GWF) module realises the simulation of a flow using a structure of model cells. In this work, a regular discretization is used that consists of layers, rows and columns. The GWF module is based on a control-volume finite-difference equation to get an approximated solution for the differential equation of the 3D movement of water through the model.

A Ground Water Transport (GWT) module is also available that simulates a 3D transport of a single solute substance in flowing water. The GWF and GWT modules are components of the MODFLOW 6 main program; they operate simultaneously during a simulation (Langevin et al., 2022).

3. HYDROLOGY OF ALPINE KARST SYSTEMS

High karst plateaus located in the Alps and around the world contain underground drainage patterns representing deep karst (Hötzl, 1992). They are dominated by kilometre-thick carbonate sequences and karstified strata, some of which extend well below the base level. The plateau systems are often surrounded by steep slopes and

Figure 1: (a) The Kanin plateau at the Slovenian-Italian border is a typical Alpine karst massif wose elevation ranges mostly between the altitudes 1800 and 2586 m a.s.l.. The vegetation cover is almost absent while numerous karst features enable a rapid infiltration of water into the underground (UTM 33N 379946 / 5135107; photo Cyril Mayaud). (b) Active ponor near Filzmoos (Hochschwab, Austria) draining water into the karst system at 1450 m a.s.l.; The two cows are potential contaminants sources and highlight the vulnerability of such features (UTM 33N 503120 / 5271243; photo Lukas Plan); (c) A 100 m deep shaft enables rapid vertical flow in the vadose zone (Steinbockschacht cave, Hochschwab, Austria, UTM 33N 508548 / 5272850; photo Ágnes Berentés); (d) A big lake/sump with an overflow in Kolowrat cave on Untersberg (Austria) as an example for a reservoir (UTM 33N 350677 / 5288003; photo Wolfgang Zillig). (e) The Kläfferquellen during snowmelt are one of the major karst springs in the Eastern Alps and drain an area of c. 70 km² (Hochschwab, Austria; UTM 33N 510938 / 5277229; drone-photo Lukas Plan).

large springs (Figure 1e) that drain extended recharge areas (Trimmel & Waltham, 2004; Plan et al., 2009; Benischke et al., 2010; Gabrovšek et al., 2023). On their top, vegetation and soils are rather scarce or even absent due to the harsh climate, while surface karst features like karren fields and dolines are generally well developed (Komac, 2001; Verres, 2010). They allow a rapid infiltration of the water, which can penetrate deep into the karst aquifer in both a diffuse and concentrated manner (Figure 1b). As part of the Alpine fold and thrust belt, the strata are subject to polyphase deformation and the tectonics is often complex. Major faults allow the development of deep vadose shafts (Figure 1c). The Hochschwab and Kanin regions are typical examples of such a configuration (Figure 1d).

4. CONCEPTUAL MODEL

To investigate the influence of the conduit geometry on the flow and transport in a simple way, the conceptual hydrogeological model representing a high Alpine karst system implemented by Plan et al. (2009) is used (Figure 2a). The innumerable subvertical structures encountered in the aquifer have a unique geometry, but are in the meantime composed of common features such as shafts, reservoirs, and constrictions that are well known

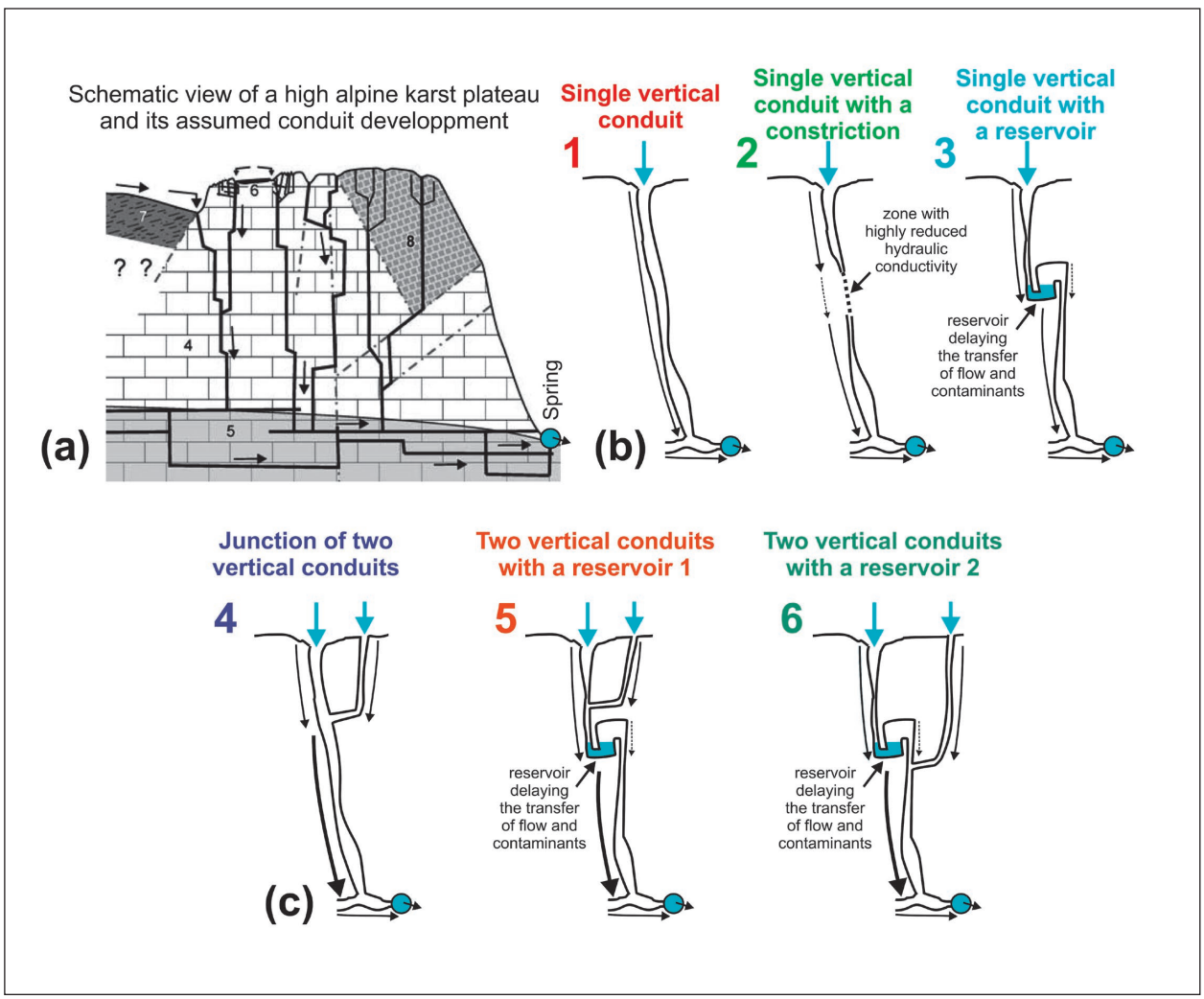

Figure 2: (a) Conceptual model showing the geometry of the vadose zone in an Alpine karst plateau (from Plan et al., 2009). Simple geometrical settings with a single shaft (b) and with two shafts (c), used for the numerical modelling. See text for details.

from cave exploration. Therefore, six vertical settings assumed to summarise the basic geometry encountered in high Alpine karst systems in a simplified way have been implemented. Three geometrical configurations with one shaft are presented in Figure 2b and three junctions of two shafts in Figure 2c:

1. *Single vertical conduit:* a vertical conduit aiming to simulate the rapid transfer of water and contaminants through the karst massif.
2. *Single vertical conduit with a constriction:* the presence of a constriction in the middle of the shaft (e.g. a plugging with fine grained sediment) is expected to dampen the transfer of water and contaminant through the karst massif.
3. *Single vertical conduit with a reservoir:* a reservoir that can be filled up to an overflow threshold is expected to control the transfer of water and contaminants. The response at the spring should be delayed as long as the level of the overflow is not reached.
4. *Junction of two vertical conduits:* this setting aims to investigate the effect of two shafts on the transfer of water and contaminants through the karst massif.
5. Two vertical conduits with a reservoir 1: this configuration aims to see the impact of two conduits on the activation of the reservoir. Their junction occurs before the reservoir.
6. *Two vertical conduits with a reservoir 2:* this setting is similar to the previous one (5), except that the junction occurs after the reservoir.

The places where concentrated infiltration occurs are shown by the blue arrows. They are aimed to represent the entrance of a shaft draining permanently or intermittently water from

its neighbouring surface area. The hypothetic transfer of water through the karst massif is materialised by the black arrows.

5. MODEL SETTINGS AND RESULTS

The six vertical settings were converted into six distributed groundwater models. Each of them is 40 m long, 30 m wide and 100 m high. This height was defined as sufficient to see the effect of the conduit geometry on the flow and transport signals. They all have a constant cell surface of 1 m^2 and are composed of seven layers. A fixed head boundary is located at a cell of the lowest layer at an elevation of 1 m, aiming to simulate the arrival of water at the model outlet at the bottom of the karst massif. The horizontal and vertical hydraulic conductivity of the karst matrix was assigned to be of 10^{-5} m/s while the cells that represent the conduits have

Table 1: Standard configuration for models with one and two input shafts.

Parameter	Value
Number of periods	80 (120s / perperiod)
Number of layers	7
Number of rows / columns	30 / 40
Column / Row width [m]	1 / 1
Top of themodel [m]	100
Hydraulic conductivity of matrix and fissures [m/s]	1e-5
Hydraulic conductivity of conduit [m/s]	1
Hydraulic conductivity of the constriction [m/s]	1e-3 / 1e-4
diffuserecharge, stress period 1 / 2-5 [m/s]	1e-10 / 1e-10
Constant head at the spring [m]	1
Concentration [kg/m^3] for continuous entry / single entry	1e-2 / 1e-1
specific storage / yield [m/s]	1e-5 / 0.35(standardvalues)
porosity	0.1

Tabe 2: Accumulated amount of recharge, discharge, mass and recovery at the constant head after a simulation run.

Type of model	Specific configuration	Total point recharge [m³]	Tracer input [kg] CI / SI	Total discharge [m³]	Tracer output [kg] CI / SI	Recovery [%] CI / SI
1. Single vertical conduit, Figure 3a		54	0.54 / 0.26	54	0.53 / 0.26	98 / 100
2. Single vertical conduit with a constriction	Kc=1e-3, Figure 3b			44	0.35 / 0.12	65 / 43
	Kc=1e-4, Figure 3c			9.7	0.032 / 0.007	5.8 / 2.7
3. Single vertical conduit with a reservoir	Overflow, Figure 3d			11.5	0.098 / 0.033	18 / 12.5
	No overflow	5.4	0.054 / 0.026	0.001	0	0
4. Junction of two vertical conduits, Figure 6a, 7a		108	0.54 / 0.26	105.9	0.47 / 0.25	87 / 95
5. Two vertical conduits with a reservoir 1	Overflow, Figure 6b, 7b			46.7	0.14 / 0.03	26 / 12.5
	No overflow			0.001	0	0
6. Two vertical conduits with a reservoir 2	Overflow, Figure 6c, 7c			65.7	0.09 / 0.033	17 / 13
	No overflow	10.8	0.054 / 0.026	5.3	0	0

a value of 1 m/s. A 2.5 hour-long hydrological event (including 10 min of autogenic recharge at the beginning) was simulated. Initially, diffuse recharge was applied onto the entire surface of the model, consisting of a portion of water with a value of 1e-10 m³/s, for a time range of 120 s (stress period), steady state (a stress period is defined as a time period with a fixed length for dividing the simulation time into defined time steps) and following 4 stress periods of transient recharge of the same value. During the next 75 stress periods, point recharge took place into the inflow points (RCH) of the models.

The model was run under steady state for the first stress period and in transient state afterwards.

To simulate transport, two different variants have been implemented beginning with stress period 6:

1. **Constant rate injection (CI):** Point recharge (RCH; e.g. entrance of input shaft or ponor) containing a constant concentration of a contaminant injected at every stress period to simulate a continuous contamination, for example caused by pasture or a leaking reservoir.
2. **Slug injection (SI):** Immediate injection of the contaminant at a single stress period while the remaining injections only contained water. This simulates a sudden input of a contaminant (e.g. fuel) or a tracer test. For the models with two shafts, additional point recharge identical to the recharge already assigned into the left shaft but without tracer were injected into the right shaft (RCH_right).

The standard model parameters (hydraulic conductivity, diffuse recharge, constant head, specific storage / yield) were taken from examples of the MODFLOW documentation and are shown in Table 1. The input parameters were derived from investigations on groundwater vulnerability of high Alpine karst plateaus (Plan et al., 2009); they are listed, together with the output values in Table 2.

5.1 SINGLE VERTICAL CONDUIT

Modelling the single vertical conduit shows an almost instantaneous water transfer from the model top to its bottom (Figure 3a, 4a). Indeed, the discharge signal recorded at the outlet is identical to the recharge that was injected at the shaft entrance. Therefore, the signal of the discharge masks the one of the recharge, which means that the two signals cannot be visually distinguished in the diagram.

According to the simple setting this result is very obvious, the concentration signal shows the expected shape for both the CI (Figure 3a) and the SI (Figure 4a). The tracer recovery of nearly 100% for both cases is also plausible.

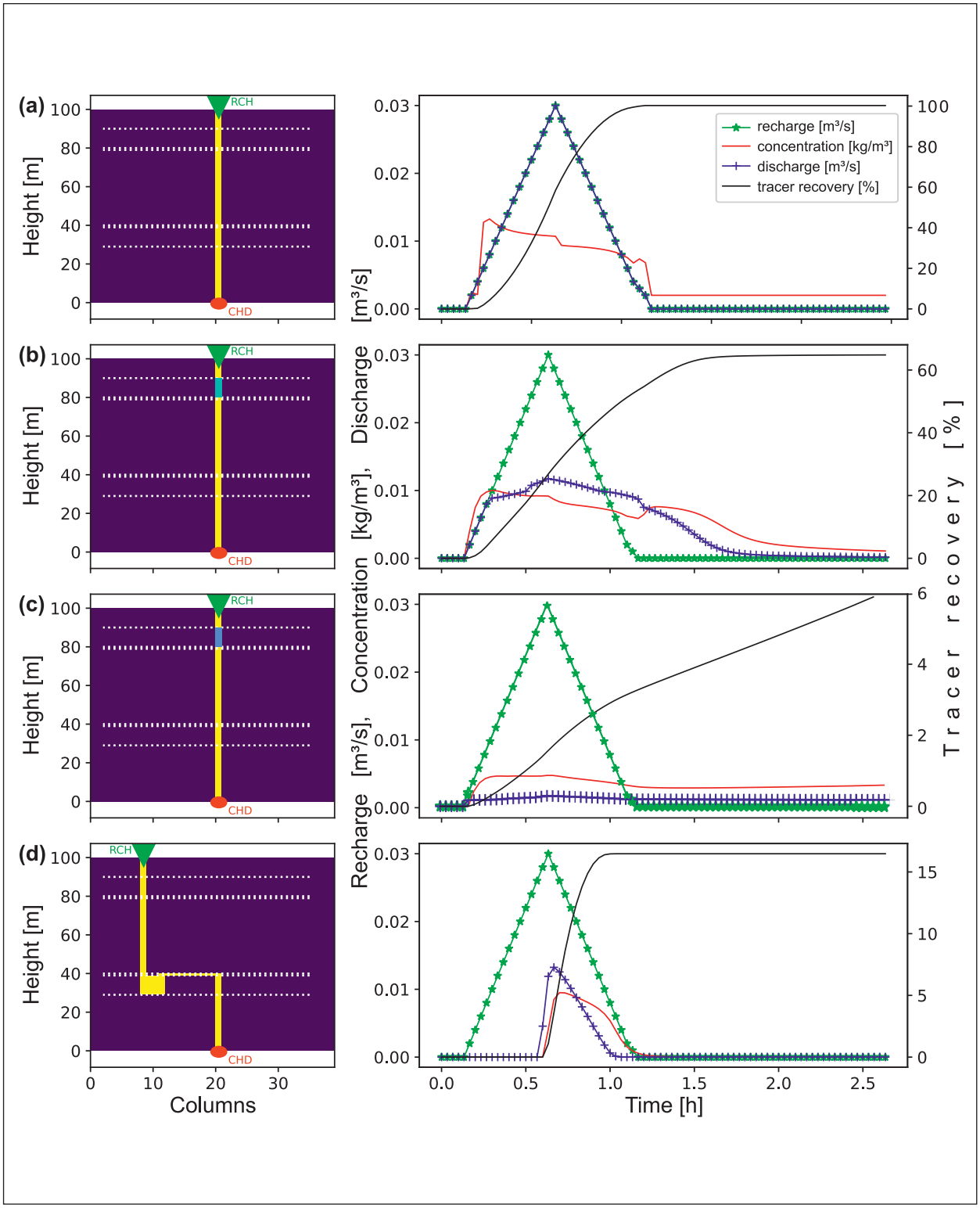

Figure 3: Models with one input shaft and continuous inflow of tracer. Models settings tested (a) single vertical conduit (model with a continuous shaft); the curves of discharge and recharge are identical, (b) single vertical conduit with a constriction with conductivity = 1e-3 (light blue), (c) single vertical conduit with a constriction with conductivity = 1e-4 (blue), (d) single vertical conduit model with a reservoir. Left: cross sections of the models at a specified row showing the conduit geometry; RCH denotes the inflow of point recharge, CHD denotes discharge at a constant head; right: Diagrams showing the values of recharge, discharge, tracer concentration, and tracer recovery.

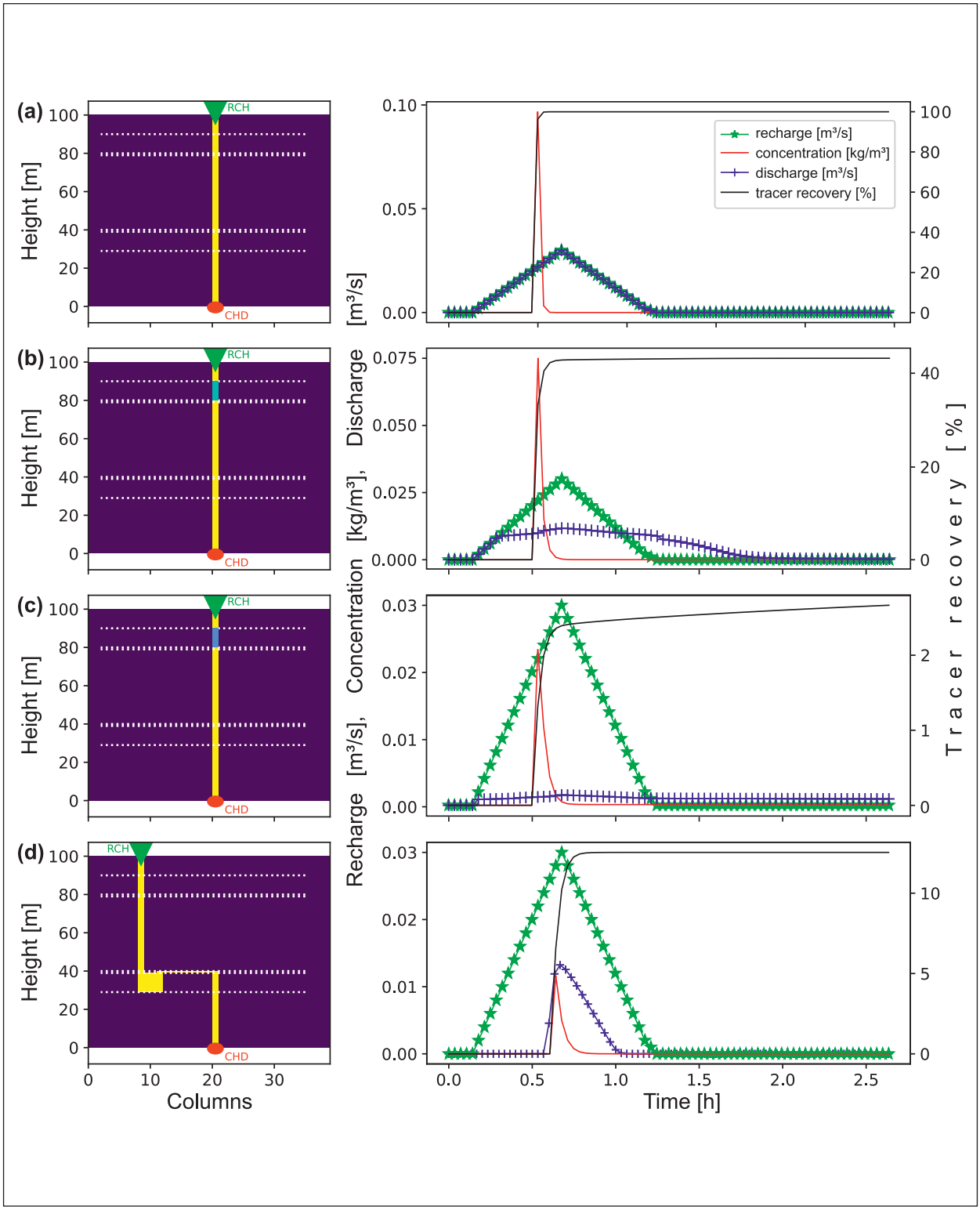

Figure 4: Models with one input shaft and immediate input of tracer. Models settings tested (a) single vertical conduit (model with a continuous shaft); the curves of discharge and recharge are identical, (b) single vertical conduit with a constriction with conductivity = 1e-3 (light blue),(c) single vertical conduit with a constriction with conductivity = 1e-4 (blue), (d) single vertical conduit model with a reservoir. Left: cross sections of the models at a specified row showing the conduit geometry; RCH denotes the inflow of point recharge, CHD denotes discharge at a constant head; right: Diagrams showing the values of recharge, discharge, tracer concentration, and tracer recovery.

5.2 SINGLE VERTICAL CONDUIT WITH A CONSTRICTION

The hydraulic conductivity of a 10 m section of the vertical conduit was reduced to simulate the presence of a constriction within the shaft (Figure 3b, c, 4b, c). In this case, two different values were tested (1e-3 m/s, 1e-4 m/s) for both injection types. As expected, both variants show reduced values for discharge, concentration and recovery values. Indeed, the discharge at the outlet was lowered up to two thirds (1e-3) and one fifth (1e-4) in amplitude and considerably dampened due to the retention effect of the constriction for both types. A similar effect was observed for the contaminant: (1) for the model with the CI the breakthrough curve was longer and flatter while the recovery rate was lower compared to the conduit without a constriction and reached 65%. (2) For the SI model the shape remained the same while the recovery was only 43%. For the second example, the conductivity value of the constriction was reduced to 1e-4 m/s, which lowered again the amplitude of both discharge and tracer signals. A recovery of 5.8% and 2.7% for CI and SI respectively was observed, showing that most of the contaminant remained retained at the constriction and some surrounding matrix cells and did not reach the model outlet at all. With the next hydrological event a supplementary amount of tracer will arrive at the outlet increasing further the recovery rate.

5.3 SINGLE VERTICAL CONDUIT WITH A RESERVOIR

To delay the transfer of water and contaminants through the system, a reservoir of 40 m³ was added to the single vertical conduit configuration (Figure 3d, 4d). As known from cave exploration, such geometrical features are frequently encountered in high Alpine karst systems (Gabrovšek et al., 2023) as well as in karst systems with less vertical development (Mayaud et al., 2014). The reservoir activation is assumed to depend on both the meteorological condition and the hydrogeological situation within the karst system. The results show that the reservoir has a strong effect on the discharge and transport curve at the model outlet (Figure 3d, 4d), with a discharge signal importantly lowered and delayed compared to the single vertical conduit. The transport behaves similarly and the arrival of the tracer at the spring is also quite reduced and depends on the activation of the overflow. The recovery rate at the end of the simulation for the CI is 18% (12.5% for the SI) which seems reasonable as most of the tracer is assumed to remain trapped in the reservoir and some surrounding matrix cells.

A further simulation aimed to test what would happen while the overflow of the reservoir would remain inactive. Therefore, the intensity of the water input was reduced by a factor of 10 (5.4 m³) compared to the standard input event. The reservoir did not reach its overflow

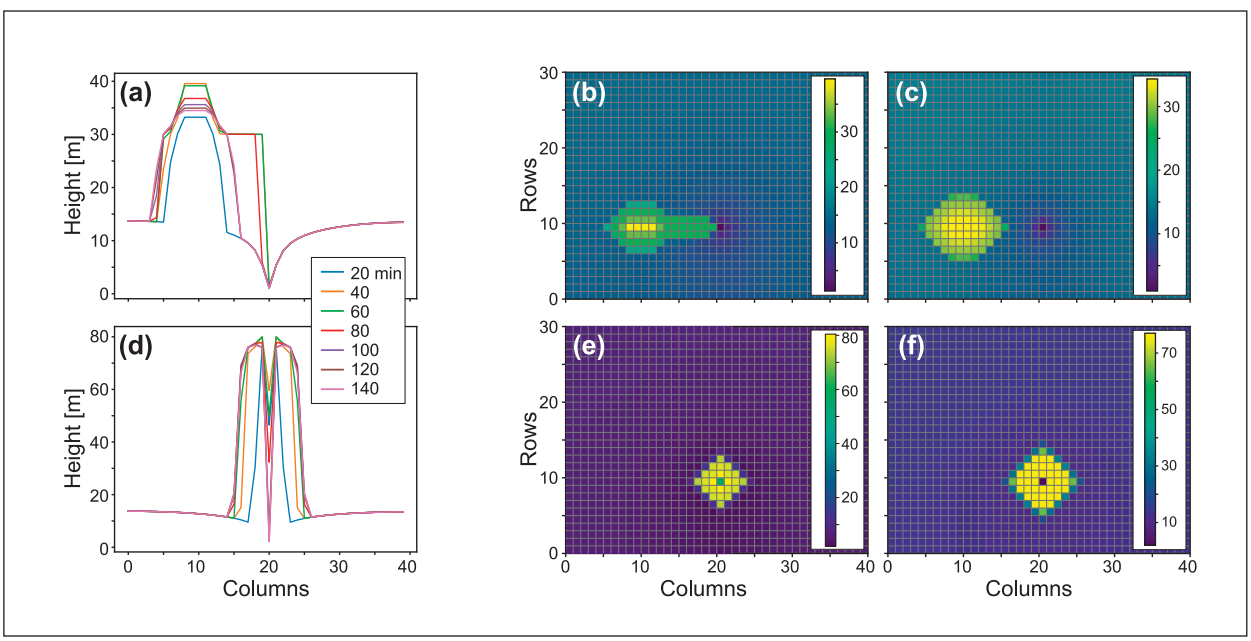

Figure 5: (a) cross section of head values at varying time steps of a model with one conduit and a reservoir; (b) Top-view of the model's head values during the simulation run after 40 minutes; the blue to yellow scale shows the head values in metres (c) Top-view of the model's head values at the end of the simulation; (d) cross section of head values at varying time steps of a model with one conduit and a constriction; (e) Top-view of the model's head values during the simulation run after 40 minutes; (f) Top-view of the model's head values at the end of the simulation.

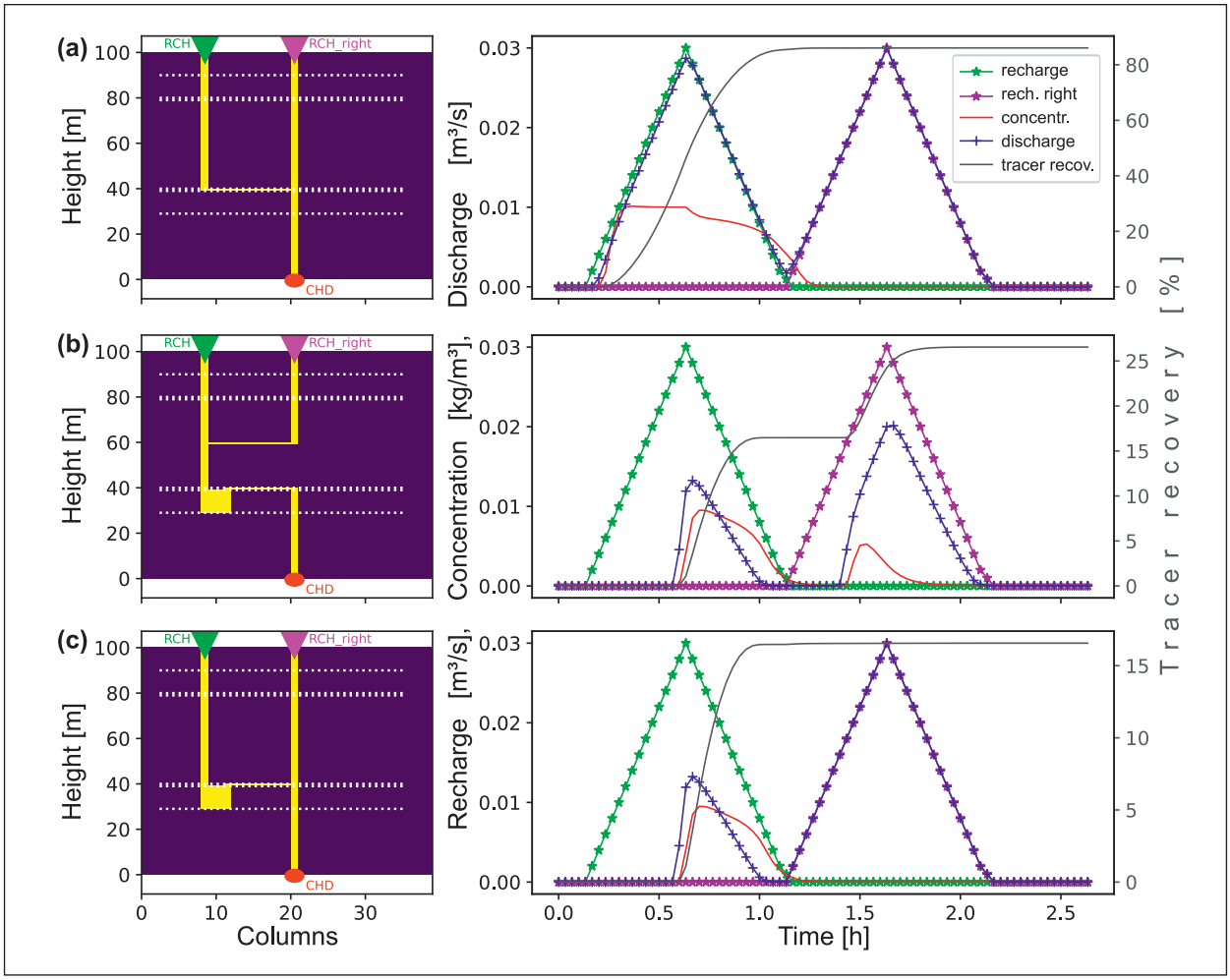

Figure 6: Models with two input shafts and continuous inflow of tracer (a) two vertical conduits, (b) two vertical conduits with a reservoir 1, swiping out the tracer by both recharge flows, (c) two vertical conduits with a reservoir 2, swiping out the tracer only from the left recharge flow; left: cross sections of the models showing the conduit geometry; RCH denotes the inflow of point recharge, CHD denotes discharge at a constant head; right: Diagrams showing the recharge, discharge, concentration, and tracer recovery.

threshold which leads to a minimal arrival of discharge at the model outlet while the concentration did not appear at all.

Figure 5 shows the head values during the simulation run of a model with a reservoir (a - c) and one with a constriction (d - f). At the cross section of the model with the reservoir, you can see the increasing values of the water level (a) corresponding to the amount of water in the model. After reaching the overflow (40 min), the water level spreads to the surrounding cells and recedes again as the amount of water decreases (80 - 140 min). (b) and (c) show the model's top views of the water levels after 40 minutes (b, highest value) and after the end of the simulation (c, lowest value). (d) shows the expansion of the water level into the surrounding cells of the constriction due to its damming effect. The top views show the head values after 40 minutes (e, highest value) and after the simulation (f, lower value but wider surroundings in the area of the conduit).

5.4 JUNCTION OF TWO VERTICAL CONDUITS

In order to study how several shafts joining together might influence the flow and transport signal, a second vertical conduit is added to the setting with a single shaft (Figure 6a, 7a) The two conduits are connected by a horizontal passage that could represent a meander, as frequently observed in caves with important vertical development. A first point recharge event is delivered into the left shaft, while a tracer is simultaneously released into the shaft for both, the CI (Figure 6a) and SI (Figure 7a). At the end of the first recharge event, a second event of similar intensity and duration but without contaminant is released into the right shaft. Results of the first event

show that the flow signal arriving at the fixed boundary is slightly modified by the presence of the horizontal conduit, which delays a bit the water transfer through the massif. The shape of the concentration signal is also modified by the horizontal passage, which smoothes its breakthrough curve for the CI case. The point recharge into the model right shaft behaves identically to the model with a single shaft with a simultaneous transfer of water through the karst massif. In addition, it can be seen that a small portion of tracer that had remained in the system arrived at the beginning of the second event only for the CI case. The total recovery rate is 87%, which is 11% less than for the single vertical conduit and can be explained by the presence of the horizontal conduit (CI) and only 5% less for the SI case.

5.5. TWO VERTICAL CONDUITS WITH A RESERVOIR 1

Because high Alpine caves usually contain all the geometrical features that were presented in the previous parts of this work, a second vertical conduit has been added to the model with the reservoir to see its potential effect on the overflow (Figure 6b, 7b). The purpose of this model is to show the behaviour of a junction of a conduit containing a reservoir with a second conduit also entering the reservoir. Similar to the delayed model, this model combination has the effect of retaining water and contaminants until a threshold is reached.

Furthermore, the water from the connected conduit also enters the reservoir and washes out the remaining tracer from the left input (CI, Figure 6b, Table 2). The right dis-

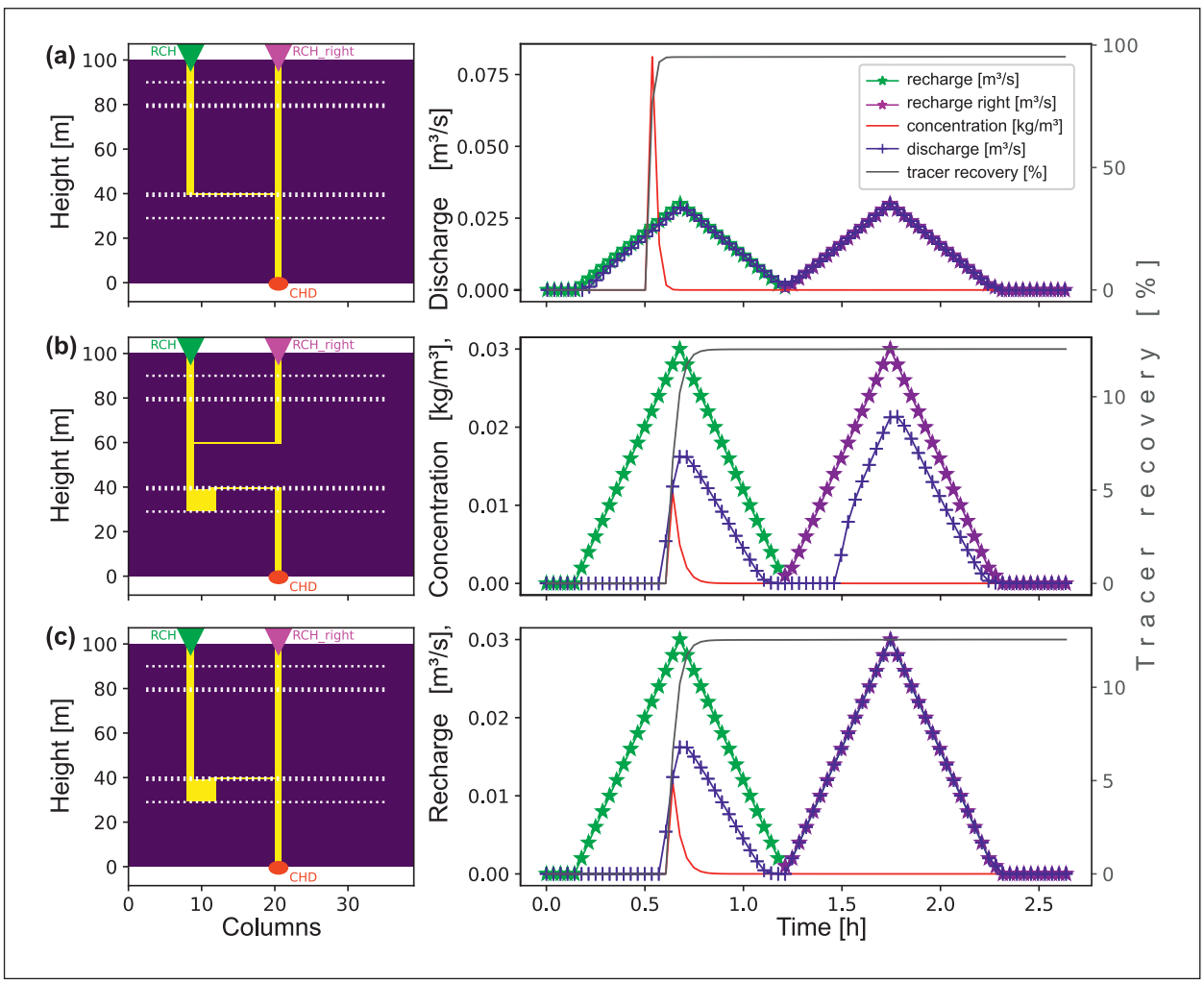

Figure 7: Models with two input shafts and immediate inflow of tracer (a) two vertical conduits, (b) two vertical conduits with a reservoir 1, second recharge flow also enters the reservoir, (c) two vertical conduits with a reservoir 2, discharge from second recharge flow similar to recharge; left: cross sections of the models at a specified row; RCH denotes the inflow of point recharge, CHD denotes discharge at a constant head; right: Diagrams showing the recharge, discharge, concentration, and tracer recovery.

charge and concentration signals also contain the rest of water and contaminants from the first event. Therefore, in contrast to the delayed model (Figure 4c), the higher recovery rate of 26% of the tracer can be seen as plausible (CI). For the SI case this influence from the second event cannot be seen, due to the less amount of tracer in the system, the recovery rate is only 12.4% similar to the delayed model.

In this case much of the tracer remains in the reservoir and also in the matrix due to the horizontal part of the conduit, compared to the single vertical conduit where nearly all of the tracer is recovered

5.6. TWO VERTICAL CONDUITS WITH A RESERVOIR 2

The purpose of this model is to show the behaviour of a junction of a conduit containing a reservoir and a second conduit connected to the outflow of the reservoir. Therefore, a model similar to the single conduit with a reservoir (Figure 4d) but with a connected conduit after the reservoir was proposed (Figure 6c, 7c). In contrast to the model shown in Figure 6b, the connected conduit at the end of the reservoir has no effect on the tracer outflow. The discharge signal yields nearly the same amount as the corresponding recharge (Figure 6c). Discharge and concentration signals show that, contrary to the model above (Figure 6b, Table 2), there is no effect from the second input signal on the tracer outflow, except a very small portion (<1%) that was stored in the matrix, therefore the small recovery rate of 17% (CI), (13% SI), similar to that of the delayed model, is plausible.

In summary, three different characteristics of the models can be recognised: (1) discharge and concentration signals are neither lowered nor delayed in a model with a single vertical conduit; (2) discharge and concentration signals are lowered but not delayed in a model with a constriction and (3) discharge and concentration signals are lowered and delayed in a model with a reservoir; for both injection types (CI and SI).

The real cases in nature are mainly assessed by the characteristic of their outflow signals like discharge and/or concentration. Therefore, they may be simulated using models with fitting behaviour as shown above.

6. DISCUSSION

In this study simple numerical models with idealised settings are used to simulate the influence of the conduit geometry of a karst aquifer on the flow and transport signals at the outlet. This approach may be applied to the simulation of a tracer test provided that suitable data is available. Tests with artificial tracers are a widely applied tool, together with detailed hydrological monitoring, to get insights into the behaviour of a karst system and are often the basis for groundwater protection investigations and aquifer modelling (e.g. Chang et al., 2019; Benischke, 2021; Schiperski et al., 2022).

The models (Figures 3 - 7, Table 2) have been developed to show the effect of the geometry on the behaviour of flow and transport. With the idealised setting (artificial, point recharge; constant tracer concentration during the whole input period (CI) or single input of tracer (SI); continuously rising recharge signal; standard values of porosity and conductivity for matrix and conduits; simple structure) the models with one or two input conduits as described in section 5 show the expected reaction. Especially, the models with a reservoir show the expected output signals of discharge, concentration, and tracer recovery value.

The simulation time of 2.5 h is sufficient to assess the behaviour of the models. The tracer that has not yet been washed out is stored in the models in the cells neighbouring the conduits and is rarely washed out, except minimum values, even if the simulation time is prolonged because there is hardly any water left in these simple models. Only a further recharge event onto an area surrounding the conduit would flush out more tracer and thus significantly increase the recovery rate.

Clearly, the hydrological conditions and the structure of the aquifer are critical to the behaviour of flow and transport signals.

Using the model with a single vertical conduit (Figure 3a, 4a) a fast flow and rapid transport of contaminants may be simulated. This behaviour is also investigated in Petrič et al. (2018). They used tracer tests to investigate the difference in discharge and transport signals due to different underground conduit geometries.

The models with a reservoir regardless of whether or not overflow conditions were reached, might simulate long-term contamination or temporarily modified aquifer boundaries depending on hydrologic situations (Maloszewski et al., 2002; Blatnik et al., 2019). Connecting the aquifer to its neighbouring recharge areas, which might occur under different contamination backgrounds was investigated in Ravbar et al. (2011). In our case, this behaviour could be simulated with the simple settings

presented above. To simulate similar examples as shown above, it would be necessary to use suitable data of tracer tests, at different hydrological situations, as application cases for the simple models to get further information of the subvertical structures of aquifers. The models show the influence of their structure on the behaviour of runoff, transport and recovery. This could make an important contribution to the GIS-based studies mentioned above that need to consider temporally and spatially constant vulnerability.

There are fundamental differences between the theoretical models shown above and use cases at natural conditions:

- Artificial point recharge only into single conduits in contrast to diffuse recharge onto the whole catchment area at precipitation events cause clear differences. This means that there is only water in the conduits and in some neighbouring cells and that the majority of the modelled cells is empty. This significantly influences the flow behaviour. Natural examples are called contact karst. There, precipitation collects on insoluble rocks and point recharge (e.g. at a ponor) occurs at the contact with the soluble karst rock (e.g. Gams, 2001).
- Standard values are used for most of the input parameters (hydraulic conductivity of matrix and conduit, porosity, specific storage and specific yield, the dimensions of the catchment area and of a reservoir) opposed to the lengthy calibration process to simulate the natural conditions of a tracer test.

For the simulation at natural conditions the conductivities of the matrix and conduits are most sensitive to calibrate the discharge, they are iteratively varied, but equifinality may occur. The simulation of the break through curve of a tracer test and the adjustment of the parameters (porosity, specific storage, and specific yield) is a lengthy process. The volume of the reservoir and the design of the conduit structure are crucial as well. The conductivities of the matrix and conduits used in numerical models are a significant simplification compared to natural conditions.

In the study of Bauer et al. (2016) it is stated, using examples from an Alpine karst massif, that the matrix and also the conduits can have many different permeabilities and porosities. There are shown fault zones containing fault cores that may be regarded as conduits with high permeability adjoining to more or less fractured rocks transitioning to solid rock with low permeability. At a regional level, it is not possible to quantify the hydrological properties with these examples. This means that there is a continuous transition from low conductivity of matrix (host rock) via fault rocks to a conduit (fault core) with high conductivity.

Nevertheless, the result of the simulation of a real case is interpretative and should be verified with different hydrologic conditions. Further studies that simulate corresponding tracer tests should take into account that the results can be integrated into GIS in order to expand the methods of vulnerability management, which have so far been constant in time and space.

We use MODFLOW 6 with EPM to simulate only laminar and no turbulent flow. The simple models, with the standard setting shown above, yield the expected behaviour. When using these models with measured data, the calibration may not provide a satisfactory result. If turbulent flow processes are not taken into account, this could lead to an overestimation of the discharge at the outlet of the karst channel (Jourde et al., 2023).

7. CONCLUSIONS

Understanding how flow and transport processes propagate through Alpine karst plateaus is challenging due to the lack of knowledge on the structure of the vertical conduit system. This work presents a set of idealised vertical settings differing in geometry, and tests of their response to simple recharge and transport signals. The numerical results allowed interpreting the flow and transport signal in the light of the model geometry.

The two variants shown, CI and SI of contamination, can provide information on: (1) the impact of pollution via one of its extreme vulnerable areas on the spring, and (2) information on the structure of the aquifer when simulating a tracer test.

These settings could be used to explain the time- and location-dependent effects of aquifers described in the introduction. Processes like long-term pollution, altered aquifer boundaries and inter-catchment flow between catchments could be explained, provided that the data from appropriate tracer tests are available. Further studies simulating corresponding tracer tests should take into account that the results need to be integrated into GIS to extend vulnerability management methods to time and space variable methods.

ACKNOWLEDGEMENTS

L.P. thanks the support by the Austrian Science Fund (FWF): P36065-N. The research of C.M. is supported within the framework of the programme Karst Research (No. P6-0119) and by the project Evaluate the impact of climate change on the groundwater reserves and ecology of a karst aquifer flooding intermittently: the Upper Pivka Valley (No. J1-60004) that are both funded by the Slovenian Research Agency (ARIS). Comments provided by two anonymous reviewers are gratefully acknowledged.

REFERENCES

Bakalowicz, M., 2005. Karst groundwater: A challenge for new resources. Hydrogeology Journal, 13: 148-160. http://doi.org/10.1007/s10040-004-0402-9

Bakker, M., Post, V., Langevin, C.D., Hughes, J.D., White, J.T., Starn, J.J., Fienen, M.N., 2016. Scripting MODFLOW Development Using Python and FloPy. Groundwater, 54(5): 733–739. https://doi.org/10.1111/gwat.12413

Ballesteros, D., Malard, A., Jeannin, P.Y., Jiménez-Sánchez, M., García-Sansegundo, J., Meléndez-Asensio, M., Sendra, G., 2015. Influence of the rivers on speleogenesis combining KARSYS approach and cave levels. Picos de Europa, Spain. In: Andreo, B., Carrasco, F., Durán, J.J., Jiménez, P., LaMoreaux, J.W., (Eds.) Hydrogeological and environmental investigations in karst systems. Springer, Berlin, pp 599–607. https://doi.org/ 10.1007/978-3-642-17435-3_67

Bauer, H., Schröckenfuchs, T.C., Decker, K., 2016. Hydrogeological properties of fault zones in a karstified carbonate aquifer (Northern Calcareous Alps, Austria). Hydrogeology Journal, 24: 1147–1170. https://doi.org/10.1007/s10040-016-1388-9

Benischke, R., Harum, T., Reszler, C., Saccon, P., Ortner, G., Ruch, C., 2010. Karstentwässerung im Kaisergebirge (Tirol, Österreich) – Abgrenzung hydrographischer Einzugsgebiete durch Kombination hydrogeologischer Untersuchungen mit Isotopenmethoden und hydrologischer Modellierung. Grundwasser, 15: 43–57. https://doi.org/10.1007/s00767-009-0124-y

Benischke, R., 2021. Advances in the methodology and application of tracing in karst aquifers. Hydrogeology Journal, 29: 67–88. https://doi.org/10.1007/s10040-020-02278-9

Blatnik, M., Mayaud, C., Gabrovšek, F., 2019. Groundwater dynamics between Planinsko Polje and springs of the Ljubljanica River, Slovenia. Acta Carsologica, 48(2): 199-226. https://doi.org/10.3986/ac.v48i2.7263

Blavoux, B., Mudry, J., Puig, J.M., 1992. The Karst System of the Fontaine de Vaucluse (Southeastern France). Environmental Geology and Water Sciences, 19: 215–225. https://doi.org/10.1007/BF01704088

Chang, Y., Wu, J., Jiang, G., Liu, L., Reimann, T., Sauter, M., 2019. Modelling spring discharge and solute transport in conduits by coupling CFPv2 to an epikarst reservoir for a karst aquifer. Journal of Hydrology, 569: 587-599. https://doi.org/10.1016/j.jhydrol.2018.11.075

Chen, Z., Auler, A.S., Bakalowicz, M., Drew, D., Griger, F., Hartmann, J., Jiang, G., Moosdorf, N., Richts, A., Stevanović, Z., Veni, G., Goldscheider N., 2017. The World Karst Aquifer Mapping project: concept, mapping procedure and map of Europe. Hydrogeology Journal, 25: 771-785. https://doi.org/10.1007/s10040-016-1519-3

Dal Soglio, L., Danquigny, C., Mazzilli, N., Emblach, C., Massonnat, G., 2020. Taking into Account both Explicit Conduits and the Unsaturated Zone in Karst Reservoir Hybrid Models: Impact on the Outlet Hydrograph. Water, 12(11): 3221. https://doi.org/doi:10.3390/w12113221

De Waele, J., Gutiérrez, F., 2022. Karst hydrogeology, geomorphology and caves. Wiley, Chichester. https://doi.org/10.1002/9781119605379

Dörfliger, N., Jeannin, P.Y., Zwahlen, F., 1999. Water vulnerability assessment in karst environments: a new method of defining protection areas using a multi-attribute approach and GIS tools (EPIK method). Environmental Geology, 39(2), 165–176. https://doi.org/10.1007/s002540050446

Duran, L., Gill. L., 2021. Modeling spring flow of an Irish karst catchment using Modflow-USG with CLN. Journal of Hydrology, 597: 125971. https://doi.org/10.1016/j.jhydrol.2021.125971.

Fleury, P., Plagnes, V., Bakalowicz, M., 2007. Modelling of the functioning of karst aquifers with a reservoir model: Application to Fontaine de Vaucluse (South of France). Journal of Hydrology, 345(1–2): 38-49. https://doi.org/10.1016/j.jhydrol.2007.07.014

Ford, D., Williams, P., 2007. Karst Hydrogeology and Geomorphology. John Wiley & Sons, pp 562. https://doi.org/10.1002/9781118684986

Gabrovšek, F., Blatnik, M., Ravbar, N., Čarga, J., Staut, M., Petrič, M., 2023. Unravelling the functioning of the vadose zone in alpine karst aquifers: new insights from a tracer test in the Migovec cave system (Julian Alps, NW Slovenia). Acta Carsologica, 52(2-3): 229-244. https://doi.org/10.3986/ac.v52i2-3.13348

Gams, I., 2001. Notion and Forms of Contact Karst. Acta Carsologica, 30(2): 33-46. URN:NBN:SI:DOC-5R3ENMZF

Goldscheider, N., Klute, M., Sturm, S., Hötzl, H., 2000. The PI method - a GIS-based approach to mapping groundwater vulnerability with special consideration of karst aquifers. Zeitschrift für Angewandte Geologie, 46(3): 157-66.

Hötzl, H., 1992. Karstgrundwasser. in: Käss, W., (Ed.). Geohydrologische Markierungstechnik, Lehrbuch der Hydrogeologie, 9: 374-406; Berlin, Stuttgart.

Jeannin, P., 2001. Modeling flow in phreatic and epiphreatic karst conduits in the Hölloch cave (Muotatal, Switzerland). Water Resources Research 37. https:// doi: 10.1029/2000WR900257. issn: 0043-1397.

Jeannin, P.Y., 2016. Main karst and caves of Switzerland. Boletín Geológico y Minero, 127(1): 45-56. https:// doi.org/10.21701/bolgeomin.127.1.003

Jourde, H., Wang, X., 2023. Advances, challenges and perspective in modelling the functioning of karst systems: a review. Environmental Earth Sciences, 82: 396. https://doi.org/10.1007/s12665-023-11034-7

Kaminsky, E., Plan, L., Wagner, T., Funk, B., Oberender P., 2021. Flow dynamics in a vadose shaft – a case study from the Hochschwab karst massif (Northern Calcareous Alps, Austria). International Journal of Speleology, 50(2): 157-172. https://doi.org/10.5038/1827-806X.50.2.2375

Kaufmann, G., 2003. Modelling unsaturated flow in an evolving karst aquifer. Journal of Hydrology, 276(1–4): 53-70. https://doi.org/10.1016/S0022-1694(03)00037-4

Kavouri, K., Dörfliger, N., Plagnes. V., Tremoulet, J., 2011. PaPRIKa: A method for estimating karst resource and source vulnerability-application to the Ouysse karst system (southwest France). Hydrogeology Journal, 19: 339–353. https://doi.org/10.1007/s10040-010-0688-8

Kavousi, A., Reimann, T., Liedl, R., Raeisi, E., 2020. Karst aquifer characterization by inverse application of MODFLOW-2005 CFPv2 discrete-continuum flow and transport model. Journal of Hydrology, 587: 124922. https://doi.org/10.1016/j.jhydrol.2020.124922

Koit, O., Ravbar, N., Marandi, A., Terasmaa, J., 2017. Threshold-controlled three-stage hydraulic behaviour of a mantled shallow carbonate aquifer (Tuhala karst area, North Estonia). Acta Carsologica, 46(2–3): 265–282. https://doi.org/10.3986/ac.v46i2-3.4951

Komac, B., 2001. The Karst Springs of the Kanin Massif. Acta Geographica, 41: 7-43.

Kordilla, J., Sauter, M., Reimann, T., Geyer, T., 2012. Simulation of saturated and unsaturated flow in karst systems at catchment scale using a double continuum approach. Hydrological and Earth System Sciences, 16: 3909–3923, https://doi.org/10.5194/hess-16-3909-2012

Kralik, M., 2001. Strategie zum Schutz der Karstwassergebiete in Österreich. BE-189. Umweltbundesamt, Vienna.

Langevin, C.D., Hughes, J.D., Banta, E.R., Niswonger, R.G., Panday, S., Provost, A.M., 2017. Documentation for the MODFLOW 6 Groundwater Flow Model: U.S. Geological Survey Techniques and Methods, book 6, chap. A55, 197 p. https://doi.org/10.3133/tm6A55

Langevin, C.D., Provost, A.M., Panday, S., Hughes, J.D., 2022. Documentation for the MODFLOW 6 Groundwater Transport Model: U.S. Geological Survey Techniques and Methods, book 6, chap. A61, 56 p. https://doi.org/10.3133/tm6A61

Lauber, U., Goldscheider, N., 2014. Use of artificial and natural tracers to assess groundwater transit-time distribution and flow systems in a high-alpine karst system (Wetterstein Mountains, Germany). Hydrogeology Journal, 22: 1807-1824. https://doi.org/10.1007/s10040-014-1173-6

Maloszewski, P., Stichler, W., Zuber, A., Rank, D., 2002. Identifying the flow systems in a karstic-fissured-porous aquifer, the Schneealpe, Austria, by modelling of environmental 18O and 3H isotopes. Journal of Hydrology, 256(1-2): 48-59.
https://doi.org/10.1016/S0022-1694(01)00526-1

Mayaud, C., Wagner, T., Benischke, R., Birk, S., 2014. Single event time series analysis in a karst catchment evaluated using a groundwater model. Journal of Hydrology, 511: 628-639. https://doi.org/10.1016/j.jhydrol.2014.02.024

Mayaud, C., Walker, P., Hergarten, S., Birk, S., 2015. Nonlinear Flow Process (NLFP): a new package to compute nonlinear flow in MODFLOW. Ground Water, 53(4): 645-650. https://doi.org/10.1111/gwat.12243

Panday, S., Langevin, C.D., Niswonger, R.G., Ibaraki, M., Hughes, J.D., 2013, MODFLOW–USG version 1: An unstructured grid version of MODFLOW for simulating groundwater flow and tightly coupled

processes using a control volume finite-difference formulation: U.S. Geological Survey Techniques and Methods, book 6, chap. A45, 66 p., https://pubs.usgs.gov/tm/06/a45.

Panday, S., 2018. USG-Transport Version 1.2.1: The Block-Centered Transport Process for MODFLOW-USG, GSI Environmental, http://www.gsi-net.com/en/software/free-software/USG-Transport.html.

Perne, M., Covington, M., Gabrovsek, F. 2014. Evolution of karst conduit networks in transition from pressurized flow to free-surface flow, Hydrology and Earth Systems Science, 18: 4617–4633. https://doi.org/10.5194/hess-18-4617-2014

Petrič, M., Kogovšek, J., Ravbar, N., 2018. Effects of the vadose zone on groundwater flow and solute transport characteristics in mountainous karst aquifers – the case of the Javorniki–Snežnik massif (SW Slovenia). Acta Carsologica, 47(1): 35-51. https://doi.org/10.3986/ac.v47i1.5144

Plan, L., Decker, K., Faber, R., Wagreich, M., Grasemann, B., 2009. Karst morphology and groundwater vulnerability of high alpine karst plateaus. Environmental Geology, 58: 285-297. https://doi.org/10.1007/s00254-008-1605-5

Plan, L., Kuschnig, G., Stadler, H., 2010. Kläffer Spring – the major spring of the Vienna water supply (Austria). In: Kresić, N., Z. Stevanović (Eds.) Groundwater Hydrology of Springs. Butterworth-Heinemann, pp. 411-427, Burlington.

Plan, L., Kaminsky, E., Oberender, P., Tenreiter, C., Wimmer, M., 2023. 4D flow pattern of the longest cave in the Eastern Alps (Schönberg-Höhlensystem, Totes Gebirge). International Journal of Speleology, 52(1): 45-56. https://doi.org/10.5038/1827-806X.52.1.2471

Ravbar, N., Goldscheider, N., 2009. Comparative application of four methods of groundwater vulnerability mapping in a Slovene karst catchment. Hydrogeology Journal, 17.3: 725-733. https://doi.org/10.1007/s10040-008-0368-0

Ravbar, N., Engelhardt, I., Goldscheider, N., 2011. Anomalous behaviour of specific electrical conductivity at a karst spring induced by variable catchment boundaries: the case of the Podstenjšek spring, Slovenia. Hydrological Processes, 25: 2130-2140. https://doi.org/10.1002/ hyp.7966

Ravbar, N., Mulec, J., Mayaud, C., Blatnik, M., Kogovšek, B., Petrič, M., 2023. A comprehensive early warning system for karst water sources contamination risk, case study of the Unica springs, SW Slovenia. Science of the Total Environment, 885: 163958. https://doi.org/10.1016/j.scitotenv.2023.163958

Reimann, T., Giese, M., Geyer, T., Liedl, R., Maréchal, J.C., Shoemaker, W.B., 2014. Representation of water abstraction from a karst conduit with numerical discrete-continuum models. Hydrological and Earth System Sciences, 18: 227–241. https://doi.org/10.5194/hess-18-227-2014

Sauro, F., Zampieri. D., Filipponi, M., 2013. Development of a deep karst system within a transpressional structure of the Dolomites in north-east Italy. Geomorphology, 184: 51-63. https://doi.org/10.1016/j.geomorph.2012.11.014

Schiperski, F., Zirlewagen, J., Stange, C., Tiehm, A., Licha, T., Scheytt, T., 2022. Transport-based source tracking of contaminants in a karst aquifer: Model implementation, proof of concept, and application to event-based field data. Water Research, 213: 118145. https://doi.org/10.1016/j.watres.2022.118145

Shoemaker, W.B., Kuniansky, E.L., Birk, S., Bauer, S., Swain, E.D., 2008. Documentation of a Conduit Flow Process (CFP) for MODFLOW-2005: U.S. Geological Survey Techniques and Methods 6-A24, 50 p. http://pubs.usgs.gov/tm/tm6a24/.

Stroj, A., Paar, D., 2019. Water and air dynamics within a deep vadose zone of a karst massif: observations from the Lukina jama–Trojama cave system (−1,431 m) in Dinaric karst (Croatia). Hydrological Processes, 33(4): 551-561. https://doi.org/10.1002/hyp.13342

Teutsch, G., Sauter, M., 1998. Distributed parameter modelling approaches in karst-hydrological investigations. Bulletin d'Hydrogéologie (Neuchâtel), 16: 99–109.

Trimmel, H., Waltham, T., 2004. Europe, Alpine. In: Gunn J (ed) Encyclopedia of caves and karst science. Routledge, New York, pp 325–327.

Veress, M., 2010. Karst Environments – Karren formation in high mountains. Springer, Heidelberg, London, New York, 230 p.

Wagner, T., Mayaud, C., Benischke, R., Birk, S., 2013. Ein besseres Verständnis des Lurbach-Karstsystems durch ein konzeptionelles Niederschlags-Abflussmodell. Grundwasser, 18(4): 225-235. https://doi.org/10.1007/s00767-013-0234-4

Živanović, V., Jemcov, I., Dragišić, V., Atanacković, N., Magazinović, S., 2016. Karst groundwater source protection based on the time-dependent vulnerability assessment model: Crnica springs case study, Eastern Serbia. Environmental Earth Sciences, 75: 1224. doi: https://doi.org/10.1007/s12665-016-6018-2

Zwahlen, F., 2004. Vulnerability and Risk Mapping for the Protection of Carbonate (Karst) Aquifers. Final Report (COST Action 620). European Commission, Directorate-General XII Science, Research and Development, Brussels, pp. 297.